

N6-methyladenine- induced LINC00667 promoted breast cancer progression through m6A/KIAA1429 positive feedback loop

Saiyu Ren^{a,b,#}, Yuxing Zhang^{b,#}, Xiaodong Yang^b, Xue Li^b, Yuexin Zheng^b, Yun Liu^b, and Xiliang Zhang ^{a,b}

^aSchool of Medicine, South China University of Technology, Guangzhou, China; ^bDepartment of General Surgery, The Sixth Medical Center of PLA General Hospital of Beijing, Beijing, China

ABSTRACT

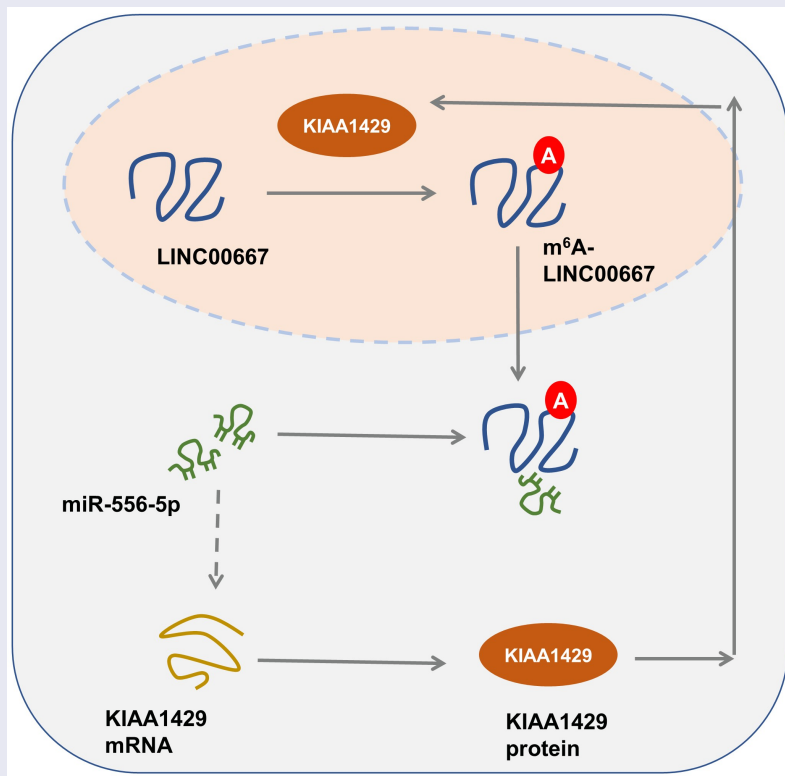
Increasing evidence supports that N⁶-methyladenine (m⁶A) and long noncoding RNAs (lncRNAs) both act as master regulators involved in breast cancer (BC) tumorigenesis at epigenetic modification level. Here, our research tries to unveil the interaction of m⁶A and lncRNAs on BC progression and explore the underlying regulatory mechanism. In the current study, we found that LINC00667 was m⁶A-modified lncRNA, which was up-regulated upon the overexpression of KIAA1429. The high expression of LINC00667 was correlated with the prognosis of BC patients. Bio-functional assays indicated that LINC00667 promoted the proliferation and migration of BC cells. Mechanistic assays illustrated that KIAA1429 targeted the m⁶A modification site of LINC00667 and enhanced its mRNA stability. Moreover, LINC00667 positively regulated the KIAA1429 via sponging miR-556-5p, forming a KIAA1429/m⁶A/LINC00667/miR-556-5p feedback loop. Collectively, the central findings of our study suggest that KIAA1429-induced LINC00667 exerted its functions as an oncogene in BC progression through m⁶A-dependent feedback loop.



ARTICLE HISTORY

Received 28 February 2022
Revised 08 May 2022
Accepted 10 May 2022


KEYWORDS

N⁶-methyladenosine; breast cancer; LINC00667; METTL3



CONTACT Xiliang Zhang  liangchua6@yeah.net  Department of General Surgery, The Sixth Medical Center of PLA General Hospital of Beijing, No. 6, Fucheng Road, Beijing, 100048, China

[#]Saiyu Ren and Yuxing Zhang are both first author.

 Supplemental data for this article can be accessed online at <https://doi.org/10.1080/21655979.2022.2077893>

© 2022 The Author(s). Published by Informa UK Limited, trading as Taylor & Francis Group.

This is an Open Access article distributed under the terms of the Creative Commons Attribution-NonCommercial License (<http://creativecommons.org/licenses/by-nc/4.0/>), which permits unrestricted non-commercial use, distribution, and reproduction in any medium, provided the original work is properly cited.

Highlights

- LINC00667 was m⁶A-induced lncRNA, which was up-regulated upon the overexpression of KIAA1429.
- LINC00667 promoted the proliferation and migration of BC cells.
- KIAA1429 targeted the m⁶A modification site of LINC00667 and enhanced its mRNA stability

1. Introduction

Human breast cancer (BC) is one of the most common cancers worldwide and the prominent leading cause of cancer-related mortality [1,2]. Despite significant clinical treatment and surgical improvements, the five-year survival rate of BC is low due to the imprecise diagnosis and untargeted treatment [3]. Currently, surgical resection combined with chemoradiotherapy still acts as the most effective therapy for advanced BC [4]. As technology advances, other novel therapies, such as molecular targeted therapy or immunotherapy, are being applied more and more in BC [5]. However, the molecular mechanism of metastatic and recurrent induced by advanced BC is still blurry. Given that the mechanism of BC progression and metastasis formation is poorly understood, there is an urgent need to investigate the mechanisms of BC progression for more precise therapeutic strategies.

N-methyladenosine (m⁶A) acts as the most prevalent internal modification on eukaryotic cells RNA [6]. Recent novel literature has reported that m⁶A modification is widespread in noncoding RNAs (ncRNAs) [7]. Besides, the m⁶A modification is written or read by the same complex in both ncRNAs and mRNAs. The m⁶A installation or uninstallation is mediated by homologous factors, namely so-called ‘writers’ or ‘erasers’ [8,9]. Moreover, the recognition of m⁶A modification is responsible by ‘readers.’ There are numerous literatures on BC having reported the function and mechanism of m⁶A. For instance, m⁶A reader YTHDF3 is clinically overexpressed in BC patients with brain metastases, and promotes the BC cell interactions with astrocytes and brain endothelial cells through enhancing the translation of m⁶A-enriched transcripts of

GJA1, ST6GALNAC5, and EGFR on their own 5'-UTR [10]. Thus, the critical roles of m⁶A on BC attract more and more attention.

Long noncoding RNAs (lncRNAs) were discovered decades ago and were identified as single-stranded RNA molecules that are more than 200 nucleotides [11,12]. Recently developed high-throughput sequencing revealed that thousands of lncRNAs were found to be highly/low expressed in a wide range of mammalian tissues. Accumulating researches have indicated that lncRNAs play a critical role in the whole process and prognosis. In BC tumorigenesis, lncRNAs regulate various pathophysiological processes. For example, lncRNA HOX transcript antisense RNA (HOTAIR) expression increases in BC tissues and cells and knockdown of HOTAIR inhibits BC cells propagation and metastasis and facilitates its apoptosis via miR-20a-5p/HMGA2 [13]. lncRNA BCRT1 is significantly upregulated in BC tissues and correlated with poor prognosis. Moreover, lncRNA BCRT1 knockdown suppresses the tumor growth and metastasis in vitro and in vivo and promotes M2 polarization of macrophages via competitively binding with miR-1303/PTBP3 axis [14]. Thus, the critical roles of lncRNAs are extremely important for BC.

In this study, we investigated the pathological roles and the underlying mechanism of m⁶A-methylated lncRNA LINC00667 in BC progression. The present research found that m⁶A-methylated LINC00667 was dramatically up-regulated in BC tissues and associated with pathological grade and poor prognosis. Moreover, we found LINC00667 was elevated by KIAA1429 via a miR-556-5p-dependent axis.

2. Materials and methods

2.1. Tissue specimens

Fifty pairs of BC tissue and paired normal tissue were gathered from the Sixth Medical Center of PLA General Hospital in Beijing from April 2018 to December 2019. The clinical data of all BC patients is shown in Table 1. All individuals with BC were diagnosed and histologically confirmed. None of the patients received any treatment prior to surgery. The Ethics Committee of the Sixth

Table 1. Correlation of LINC00667 expression with BC patients' clinicopathological feature.

	LINC00667			P value
	Total	High	Low	
Age (years)				
≥50	23	13	10	0.394
<50	27	12	15	
Lymph metastasis				
No	22	8	14	0.087
Yes	28	17	11	
Tumor size				
≥2 cm	37	23	14	0.003
<2 cm	13	2	11	
TNM				
I-II	30	17	13	0.248
III-IV	20	8	12	
Differentiation				
Well, moderate	29	14	15	0.774
Poor	21	11	10	
ER status				
Positive	19	11	8	0.560
Negative	31	14	17	
PR status				
Positive	20	10	10	0.999
Negative	30	15	15	
Her-2 status				
Positive	12	5	7	0.741
Negative	38	20	18	

*P < 0.05 represents statistical difference.

Medical Center of PLA General Hospital in Beijing was authorized and approved. The agreement and informed consent were obtained from every participator.

2.2. Cell lines

Human normal breast epithelial cell (MCF-10A) and BC cell lines (MCF-7, MDA-MB-468, and MDA-MB-231) were purchased from American Type Culture Collection (ATCC, Manassas, VA, USA) and cultured in Dulbecco's modified Eagle's medium (DMEM, Corning, USA) supplemented with 10% fetal bovine serum (FBS; Gibco, USA) and penicillin-streptomycin solution (Gibco, USA) at 5% CO₂ cell culture under 37°C.

2.3. Transfection

The cDNA of LINC00667 was PCR-amplified and subcloned into pcDNA 3.1 (+) vector (Invitrogen). Then, the antisense LINC00667 was subcloned into the pcDNA3.1 (-) vector (Invitrogen), named as pcDNA3.1-antisense-LINC00667. For the silencing of LINC00667, the shRNA and their respective

controls were provided from GeneScript (Nanjing, China). All products were validated by DNA sequencing. The BC cells were infected with lentivirus with 5 mg/mL polybrene, and after 48 h, 2 mg/mL puromycin was added to the culture medium to select the infected cells. The sequences of oligonucleotides used in the present study are shown in **Table S1**.

2.4. Quantitative real-time PCR

Total RNA was extracted from clinical BC specimens or BC cells using TRIzol reagent (Invitrogen) according to the protocols. The first-strand cDNA was then synthesized using PrimeScript RT Reagent Kit (Takara, Otsu, Japan). Then, quantitative real-time PCR was performed on the ABI7500 system using SYBR Green methods. The relative mRNA or lncRNA expression was measured normalized to GAPDH by the 2^{-ΔΔCT} method.

2.5. Cell viability assay

For CCK-8 assay, transfected BC cells (1.0 × 10³/well) were seeded into 96-well plate and incubated with a Cell Counting Kit 8 (CCK-8) solution (Apexbio, Houston, TX, USA) for 4 h. The absorbance at 450 nm was observed using a microplate reader (Bio-Rad, Hercules, CA, USA). For cell cycle analysis, after transfection, BC cells were washed with PBS and fixed by 70% ethanol at 4°C for 2 h. DNA was stained by 10 mg/mL propidium iodide (PI) and DNase-free RNase (Roche Diagnostics) PBS for 30 min. Flow cytometry was carried out using Coulter EPICS XL Flow Cytometer (Beckman Coulter, Inc., Fullerton, CA) with Modified software (BD Biosciences).

2.6. Western blot

BC cells were lysed in a buffer of ice-cold RIPA lysis (Beyotime Biotechnology, China) added with protease inhibitors. The protein concentration was measured with the Rapid Gold BCA Protein Assay Kit (Thermo Fisher Scientific, Waltham, MA, USA). An equal amount of protein was placed on the SDS-PAGE gel and then electrophoretically transferred to polyvinylidene fluoride (PVDF) membranes. Primary antibodies (anti-VIRMA,

1:1000, Cell Signaling Technology, catalog no. 88358; anti-m⁶A antibody, catalog no. ab208577, 1:1000, Abcam) were used in this study, as well as second antibodies anti-beta-actin (catalog no. 4970, Cell Signaling Technology).

2.7. Migration assays

Transwell migration assays were carried out by chamber (8 μ m pore, BD Biosciences). In these assays, 2×10^4 cells in a serum-free DMEM medium (200 μ l) were added to the top chamber and medium with 10% fetal bovine serum (600 μ l, Gibco) was added to the lower chamber. After 24-h incubation at 37°C, the migrated cells to the lower chamber were fixed by 4% paraformaldehyde for 30 min and then stained with crystal violet (1%) at room temperature for 2 h. The stained cells were counted in five different and random fields under inverted microscope (Olympus Corporation, Tokyo, Japan).

2.8. Cellular sublocation analysis

Cellular location was performed using PARIS Kit (Invitrogen, Carlsbad, CA, USA) following the manufacturer's protocol. Briefly, the nuclear and cytoplasmic fractions were isolated and finally calculated using RT-PCR. U1 snRNA and GAPDH were employed as positive control for nuclear and cytoplasmic fractions, respectively.

2.9. RNA immunoprecipitation (RIP)

RIP analysis was performed using Magna RIP RNA-Binding Protein Immunoprecipitation kit (Millipore, Billerica, MA, USA) instructions. BC cells were lysed with a lysis buffer (100 mL) containing a protease inhibitor and a ribonuclease inhibitor for 30 min on ice with centrifugation (257,643 g, 5 min, 4°C). Then, the supernatant acted as an input (positive control). IgG and protein-specific antibody (anti-m⁶A, anti-AGO2) and 50 mL protein A/G-beads were added to the supernatant. The sample was rotated and incubated overnight following centrifugation at 4°C. Protein A/G-bead precipitation was washed three times. Subsequently, the sample was added with SDS loading buffer. The

relative RNA in the precipitation after isolation and purification was verified by qRT-PCR.

2.10. Luciferase reporter assay

The sequences of LINC00667 and KIAA1429 mRNA 3'-UTR sequences containing miR-556-5p complementary sites were cloned into pGL3-control luciferase reporter vectors (Promega, Madison, WI, USA), which were named LINC00667-WT or KIAA1429-WT, respectively. The mutate sites were named as LINC00667-MUT or KIAA1429-MUT, respectively. 293T cells were co-transfected with WT or MUT together with miR-556-5p or miR-NC. After 24-h transfection, a luciferase reporter system (Promega) was performed to assess luciferase activity.

2.11. m⁶A quantification

Quantification of m⁶A RNA methylation was detected by m⁶A RNA methylation assay kit (catalog no. ab185912, Abcam) following the manufacturer's protocols. A total RNA sample (400 ng) for each group determined the m⁶A percentage. Absorbance at 450 nm was measured by a microplate reader, and the percentage of m⁶A in total RNA was calculated.

2.12. RNA stability assay

BC cells were transfected and then seeded in 6-well plates. After 24-h transfection, BC cells were treated with actinomycin D (5 μ g/mL, catalog no. HY-17559) for 0 h, 3 h, and 6 h before collection. Total RNA was isolated for RT-PCR analysis.

2.13. Methylated RNA immunoprecipitation (MeRIP)-qPCR

MeRIP-PCR assay for gene's m⁶A modification was performed using Magna MeRIP Kit (catalog no. CR203146, Millipore, Massachusetts, USA) according to the manufacturer's instructions. In brief, BC cells were washed with ice-cold PBS twice and then harvested for collection by centrifugation (1500 rpm, 4°C, 5 min). Removing the supernatant, the cells were mixed with 100 μ L RIP lysis buffer and incubated on

ice for 5 min. Anti-mA antibody (5 μ g) was coated to magnetic beads and washed with RIP washing buffer twice and resuspended (RIP immunoprecipitation buffer 900 μ L + 100 μ L cell lysate). After overnight at 4°C, beads were washed and extracted for RNA enrichment analysis by qRT-PCR.

2.14. Xenograft tumorigenesis model

Five-week-old BABL/c nude mice (12 mice) were provided by Beijing Vital River Laboratory Animal Technology Limited Company (Beijing, China). MDA-MB-231 cells (5×10^6) were subcutaneously injected into the flanks of mice. The tumor volume was assessed according to the tumor weight and length for 3 weeks using a standard formula: length \times width²/2. After sacrificing the mice, xenograft tumors were harvested and the tumor weight was calculated. All animal studies were approved by the Animal Care and Use Committee of the Sixth Medical Center of PLA General Hospital in Beijing.

2.13. Statistical analysis

The data are presented as the mean \pm SD value. Data analysis was plotted using GraphPad Prism 8.0. One-way ANOVA following Tukey's post hoc test was performed for comparisons of more than two groups. Paired two-tailed Student's t-tests were performed for comparisons between the two groups. Correlations between different factors (KIAA1429, LINC00667) expression levels of were assessed by Spearman correlation analysis. Survival analysis was analyzed using the log-rank test and plotted using Kaplan–Meier survival curves. All experiments were repeated at least three times. Difference of $P < 0.05$ was considered significant.

3. Results

LINC00667 was m⁶A-modified lncRNA, which was up-regulated upon the overexpression of KIAA1429. The high expression of LINC00667 was correlated with the prognosis of BC patients. Bio-functional assays indicated that LINC00667 promoted the proliferation and migration of BC cells. Mechanistic assays illustrated that KIAA1429 targeted the m⁶A modification site of LINC00667 and enhanced its mRNA stability. Moreover,

LINC00667 positively regulated the KIAA1429 via sponging miR-556-5p, forming a KIAA1429/mA/LINC00667/miR-556-5p feedback loop.

3.1. LINC00667 was an m⁶A-related lncRNA up-regulated in BC

The dataset information suggested that KIAA1429 up-regulated in the BC cohort (Figure 1a). Our research constructed KIAA1429 overexpression stable transfection cells (MCF-7 cells) and then the potentially dysregulated lncRNAs were detected. Results indicated that numerous lncRNAs were dysregulated upon KIAA1429 overexpression (Figure 1b). Then, we calculated three candidate lncRNAs (LINC00667, CASC9, and LINC00958) using RT-PCR, showing that LINC00667 significantly up-regulated in KIAA1429 overexpression (Figure 1c). Correlations between of KIAA1429 and LINC00667 expression showed that KIAA1429 positively correlated with the LINC00667 (Figure 1d). The above results demonstrated that LINC00667 was an m⁶A-related lncRNA up-regulated in BC.

3.2. LINC00667 acted as an oncogenic factor for BC

In the enrolled BC tissue samples, the analysis illustrated that LINC00667 levels were up-regulated in the BC samples (Figure 2a). In BC cell lines (MCF-7, MDA-MB-468, and MDA-MB-231), the LINC00667 level was also increased as compared to normal breast epithelial cell (MCF-10A) (Figure 2b). The BC cohort was divided into a high-expression group and a low-expression group according to LINC00667 mean value (Figure 2c). Kaplan–Meier survival curves by log-rank test suggested that high LINC00667 level indicated a poorer prognosis (Figure 2d). The above results demonstrated that LINC00667 acted as an oncogenic factor for BC.

3.3. KIAA1429 elevated the enrichment of lncRNA LINC00667

Using the m⁶A online tool (<http://www.cuilab.cn/sramp>), a sequence-based N-methyladenosine (m⁶A) modification site predictor, we found that there were several m⁶A sites on the LINC00667 sequence

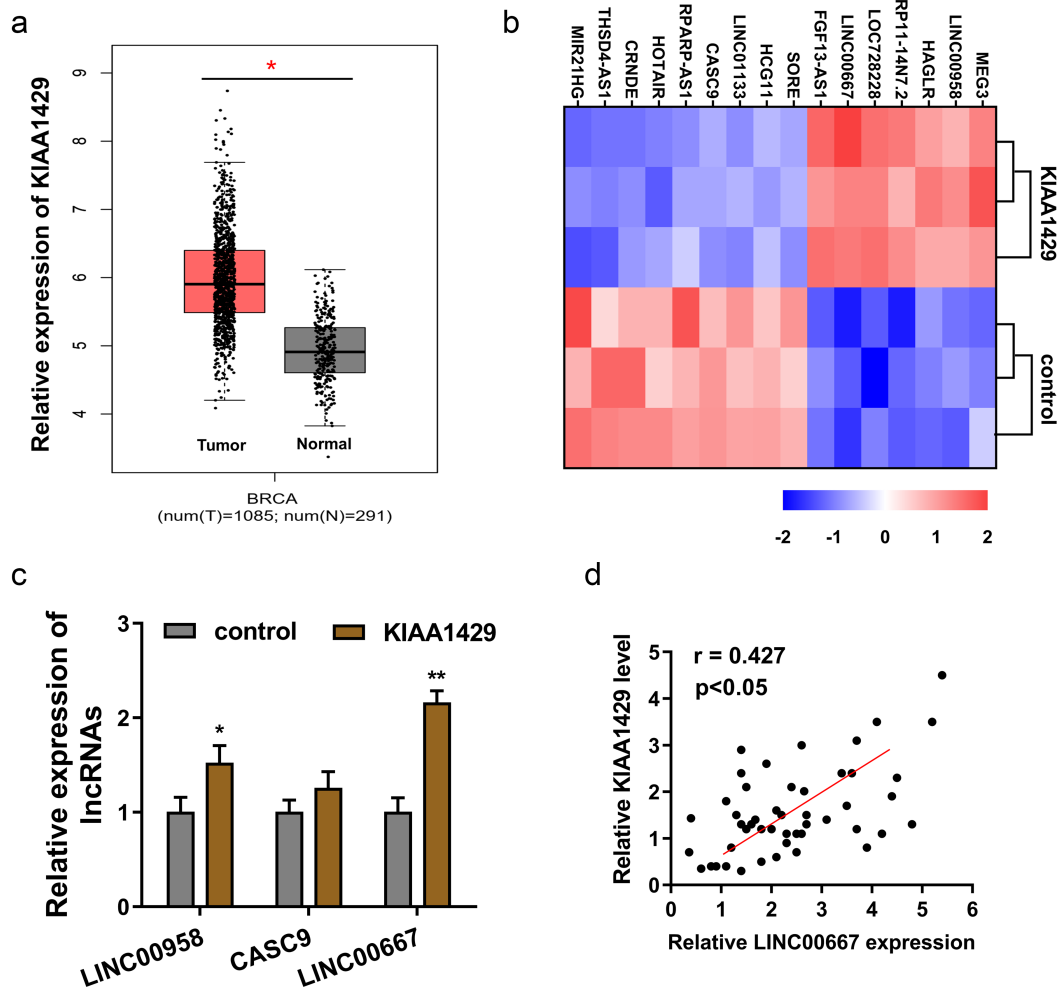


Figure 1. LINC00667 was an m⁶A-related lncRNA up-regulated in BC. (a) The GEPIA dataset (gene expression profiling interactive analysis, <http://gepia.cancer-pku.cn/index.html>) suggested the up-regulation of KIAA1429 in the BC cohort. (b) Heatmap showed the dysregulated lncRNAs in MCF-7 cells transfected with KIAA1429 overexpression or control. (c) Three candidate lncRNAs (LINC00667, CASC9, and LINC00958) were determined using RT-PCR. (d) Correlations between KIAA1429 and LINC00667 expression was assessed by Spearman correlation analysis. * $P < 0.05$; ** $P < 0.01$.

(Figure 3a). Then, we constructed an overexpression transfection of KIAA1429 in BC cells (Figure 3b). RT-PCR assays indicated that LINC00667 level was significantly up-regulated in the KIAA1429-overexpressed cells (Figure 3c). m⁶A quantitative analysis illustrated that the m⁶A enrichment was up-regulated in the KIAA1429 overexpressed cells (Figure 3d). Further analysis found that the m⁶A-modified sites on the LINC00667 sequence were TGACC (Figure 3e). MeRIP-PCR assay demonstrated that the m⁶A level was up-regulated in LINC00667 (Figure 3f). RNA stability assay illustrated that KIAA1429 overexpression promoted the enrichment of lncRNA LINC00667 (Figure 3g). Overall, these findings suggested that KIAA1429 elevated the

enrichment of lncRNA LINC00667 via m⁶A-dependent manner.

3.4. lncRNA LINC00667 promoted the progression of BC

Bio-function assay was performed using MDA-MB-231 (for LINC00667 overexpression) and MCF-7 (for LINC00667 knockdown) cells (Figure 4a). CCK-8 assays suggested that LINC00667 overexpression promoted the proliferation, and LINC00667 knockdown repressed the proliferation (Figure 4b). Migration assay by transwell indicated that LINC00667 overexpression promoted the migration, while LINC00667 knockdown repressed the

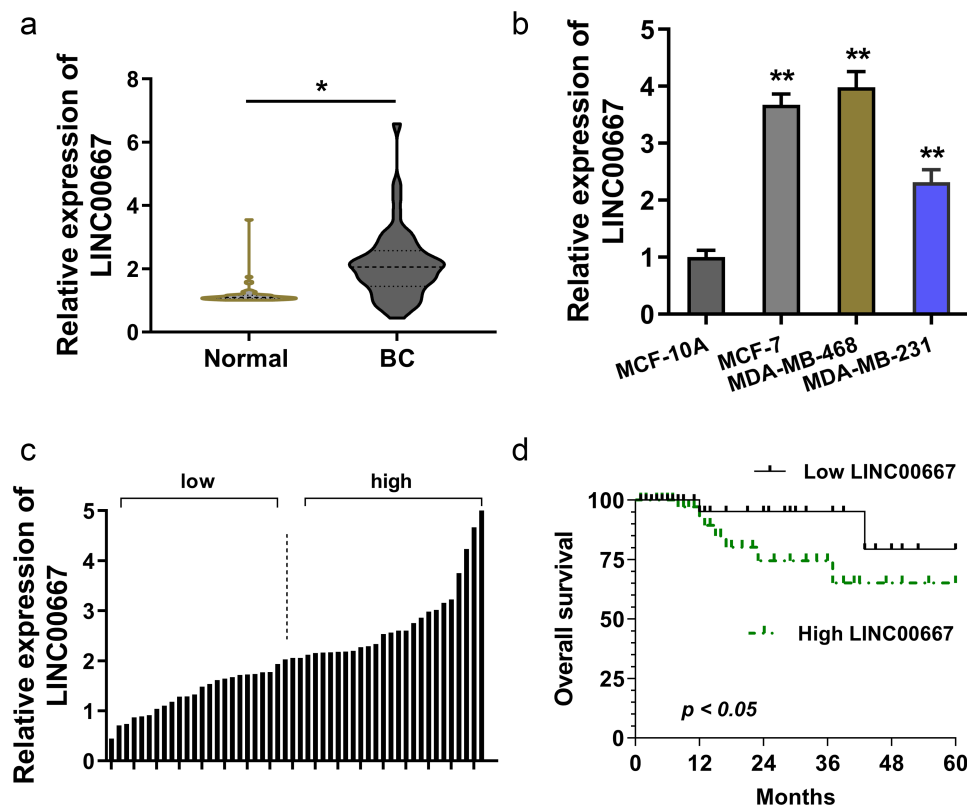


Figure 2. LINC00667 acted as an oncogenic factor for BC. (a) LINC00667 levels were determined using RT-PCR in the enrolled BC samples. (b) LINC00667 levels were determined using RT-PCR in the BC cell lines (MCF-7, MDA-MB-468, and MDA-MB-231) and normal breast epithelial cell (MCF-10A). (c) The BC cohort was divided into high-expression group and low-expression group according to LINC00667 mean value. (d) Kaplan–Meier survival curves by log-rank test showed the prognosis of BC patients. * $P < 0.05$; ** $P < 0.01$.

migration (Figure 4c). Cell cycle analysis suggested that LINC00667 overexpression accelerated the cycle progression, while LINC00667 knockdown arrested the cycle at G1/S phase (Figure 4d). In vivo xenograft assay suggested that LINC00667 overexpression facilitated the tumor growth in mice with subcutaneous transplantation (Figure 4e). Overall, these findings showed that lncRNA LINC00667 promoted the progression of BC.

3.5. LINC00667 targeted the miR-556-5p/KIAA1429 axis in BC

In the BC cells (MDA-MB-231, MCF-7), subcellular analysis found that LINC00667 mainly located in the cytoplasm of BC cells (Figure 5a). Then, we investigated the potential downstream miRNAs for LINC00667, and results suggested that miR-556-5p showed a good matching for LINC00667 (Figure 5b). Luciferase reporter assays indicated that miR-556-5p closely correlated with LINC00667 3'-UTR

(Figure 5c). Ago2-RIP assay illustrated that miR-556-5p interacted with LINC00667 at molecular level (Figure 5d). Online tools (miRanda, PITA, and TargetScan) suggested that KIAA1429 acted as the downstream target of miR-556-5p (Figure 5e). The wild type and mutant of luciferase vectors for KIAA1429 mRNA were constructed (figure 5f). Results of luciferase reporter assays illustrated that miR-556-5p closely correlated with KIAA1429 mRNA 3'-UTR (Figure 5g). Western blot assay suggested that LINC00667 could positively regulate the protein level of KIAA1429 (Figure 5h). These data indicated that LINC00667 targeted the miR-556-5p/KIAA1429 axis, moreover, forming a KIAA1429/LINC00667/miR-556-5p feedback loop (Figure 6).

4. Discussion

Due to the rapid development of high-throughput sequencing technology and bioinformatics, the role of m⁶A and lncRNAs is attracting more and

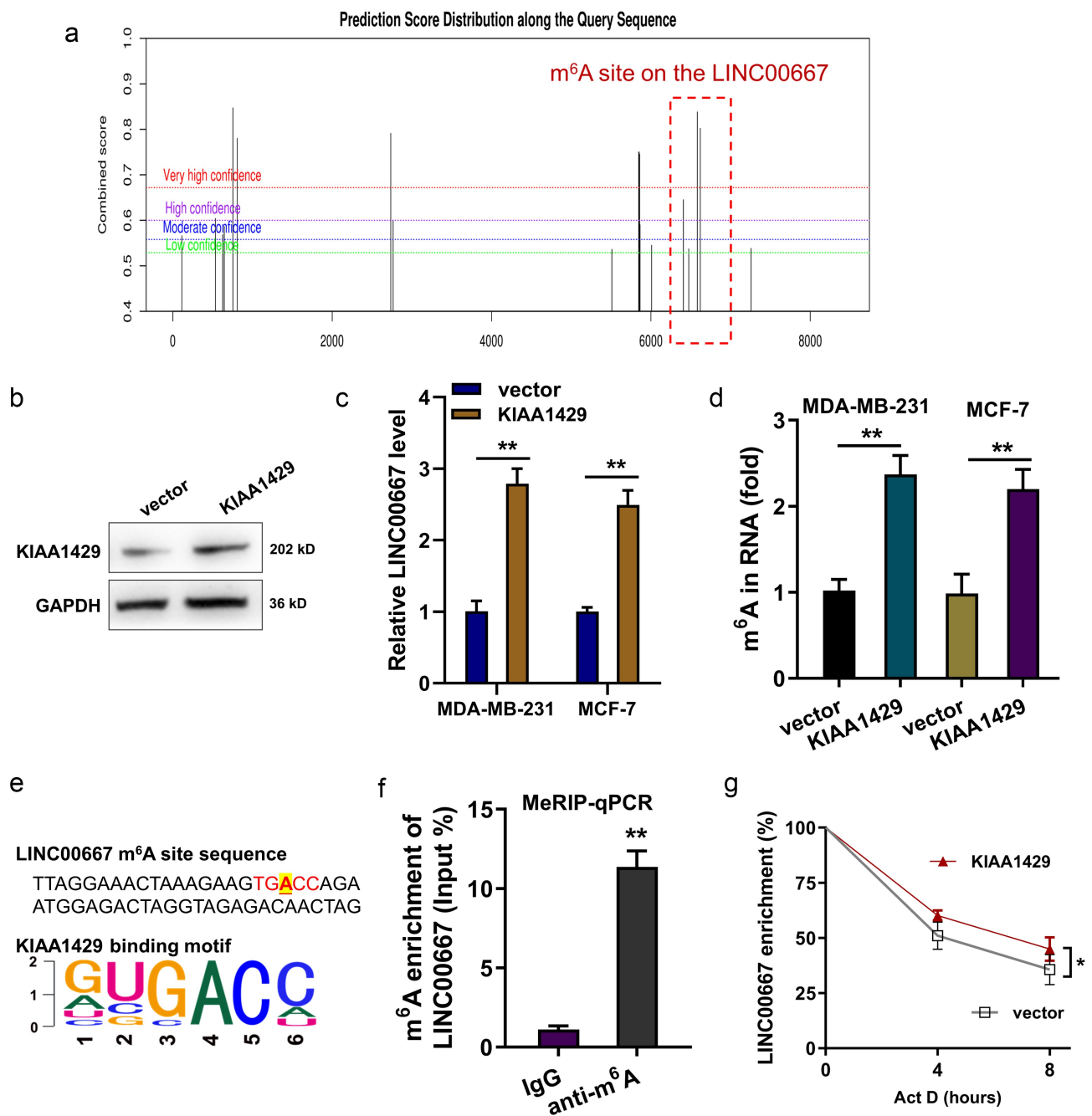


Figure 3. KIAA1429 elevated the enrichment of lncRNA LINC00667. (a) m⁶A online tool (<http://www.cuilab.cn/sramp>), a sequence-based N⁶-methyladenosine (m⁶A) modification site predictor, showed the m⁶A sites on the LINC00667 sequence. (b) Overexpression of KIAA1429 was transfected in BC cells. Western blot showed the transfection efficiency. (c) RT-PCR assays indicated the LINC00667 level in the KIAA1429 overexpressed cells. (d) m⁶A quantitative analysis illustrated the m⁶A enrichment in the KIAA1429 overexpressed cells. (e) The m⁶A-modified sites on the LINC00667 sequence were TGACC. (f) MeRIP-PCR assay demonstrated the m⁶A level in LINC00667. (g) RNA stability assay illustrated the enrichment of lncRNA LINC00667 upon KIAA1429 overexpression. * $P < 0.05$; ** $P < 0.01$.

more attention for researchers [15,16]. Recently, numerous lncRNAs have acted as critical modulators in various biological processes in human

cancer. Compared to mRNAs, lncRNAs are also abundantly expressed in BC. The chemical internal modification on eukaryotic messenger RNAs

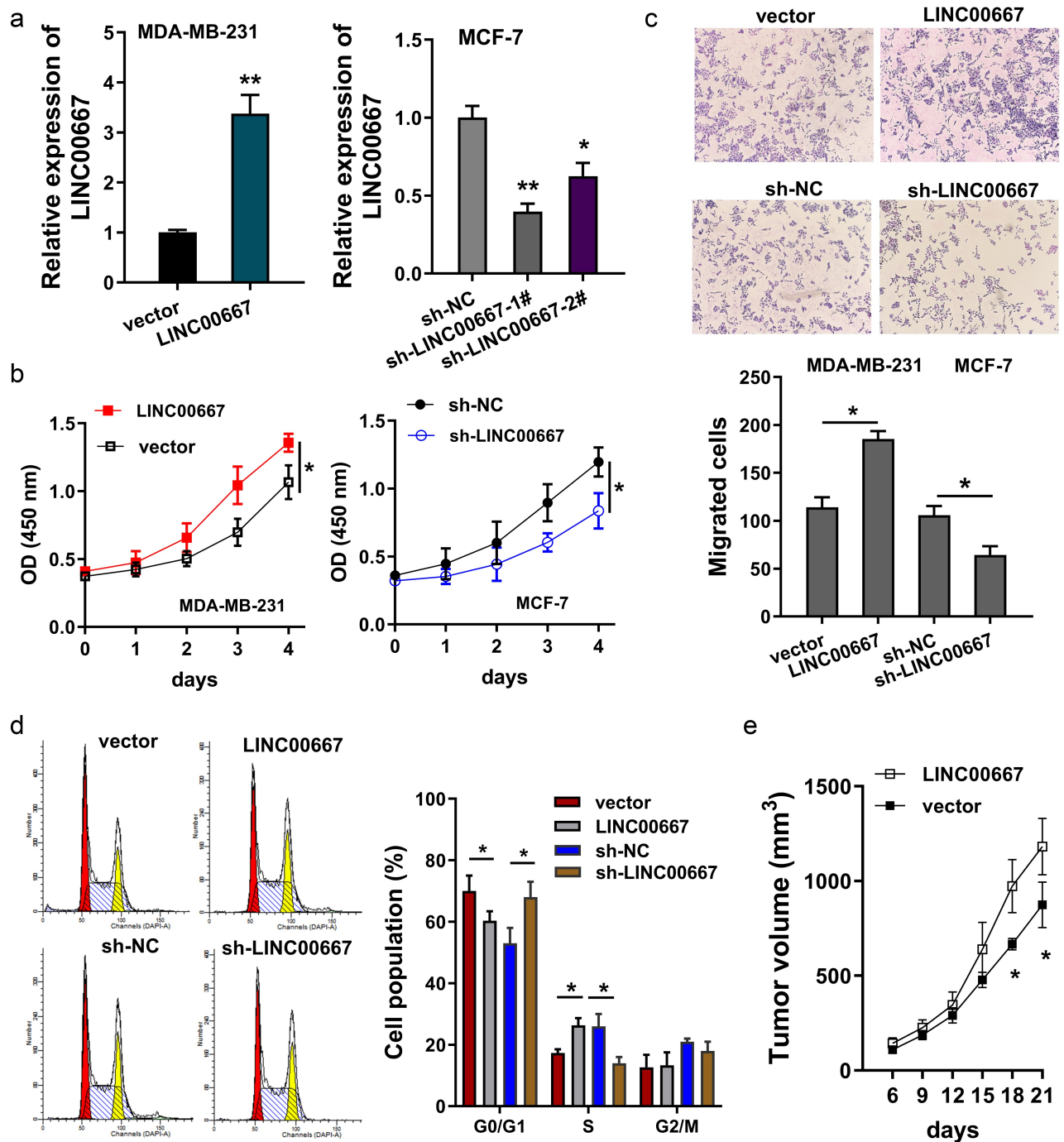


Figure 4. LncRNA LINC00667 promoted the progression of BC. (a) RT-PCR determined the LINC00667 level in MDA-MB-231 (for LINC00667 overexpression) and MCF-7 (for LINC00667 knockdown) cells. (b) CCK-8 assays determined the proliferation of MDA-MB-231 with LINC00667 overexpression and MCF-7 cells with LINC00667 knockdown. (c) Migration assay by transwell indicated the migration of MDA-MB-231 with LINC00667 overexpression and MCF-7 cells with LINC00667 knockdown. (d) Flow cytometry for cell cycle analysis showed the cycle progression of MDA-MB-231 and MCF-7 cells. (e) In vivo xenograft assay showed the tumor growth in mice subcutaneous transplantation with LINC00667 overexpression. * $P < 0.05$; ** $P < 0.01$.

dramatically changes the fate of RNAs [17]. In addition to this, the m⁶A modification on lncRNA also enriches the biological functions of lncRNAs in cancers.

In the present study, we found that the LINC00667 was an m⁶A-related lncRNA with high expression in KIAA1429 overexpression transfection. Moreover, KIAA1429 could install the m⁶A modification on

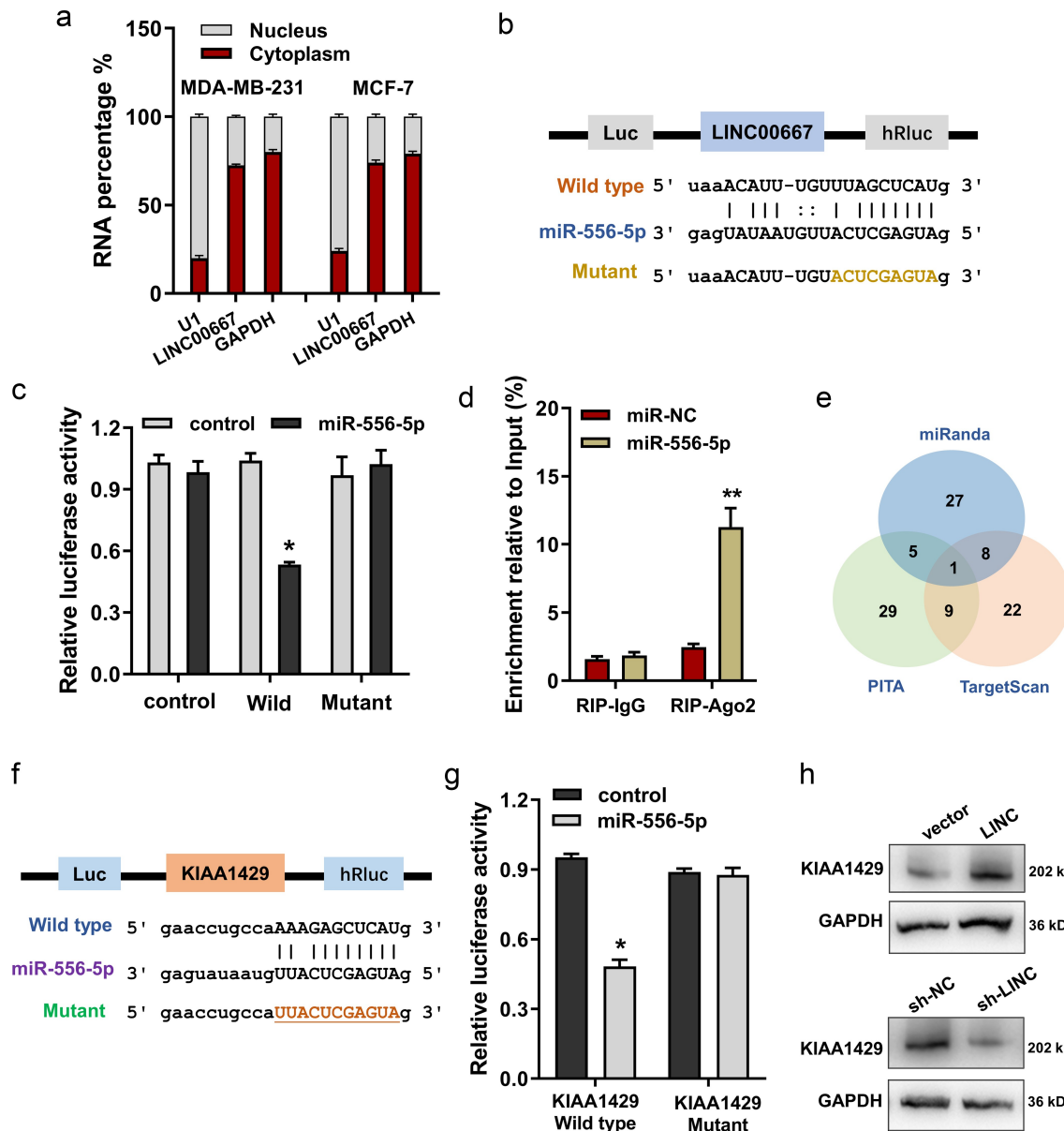


Figure 5. LINC00667 targeted the miR-556-5p/KIAA1429 axis in BC. (a) Subcellular analysis revealed the cytoplasm location of LINC00667 for BC cells (MDA-MB-231, MCF-7). (b) miR-556-5p showed a well matching binding for LINC00667. Wild type and mutant sequences at 3'-UTR were constructed. (c) Luciferase reporter assays indicated the close correlation within miR-556-5p and LINC00667. (d) Ago2-RIP assay illustrated the interaction within miR-556-5p and LINC00667. (e) Online tools (miRanda, PITA, TargetScan) suggested the downstream target of miR-556-5p. (f) The wild type and mutant of luciferase vectors for KIAA1429 mRNA were constructed. (g) Luciferase reporter assays illustrated the close correlation within miR-556-5p and KIAA1429 mRNA 3'-UTR. (h) Western blot assay suggested the protein level of KIAA1429 upon LINC00667 overexpression or knockdown. * $P < 0.05$; ** $P < 0.01$.

the 3'-UTR of LINC00667. The interaction within m⁶A and lncRNA is a novel research hotspot. For instance, in BC, m⁶A methyltransferase METTL3 up-regulates the level of MALAT1 by modulating its m⁶A modification, and moreover, MALAT1 promotes the expression of HMGA2 by sponging miR-26b. Thus, METTL3 promotes BC tumorigenesis via MALAT1/miR-26b/HMGA2 axis [18]. LncRNA

DLGAP1 antisense RNA 1 (DLGAP1-AS1) is an up-regulated mA-related lncRNA that is overexpressed in adriamycin-resistant BC cells. M⁶A methyltransferase binds to the m⁶A-modified site of DLGAP1-AS1 and motivates its stability through WTAP/DLGAP1-AS1/miR-299-3p feedback loop [19]. Thus, it can be seen that m⁶A-related lncRNA participates in tumorigenesis.

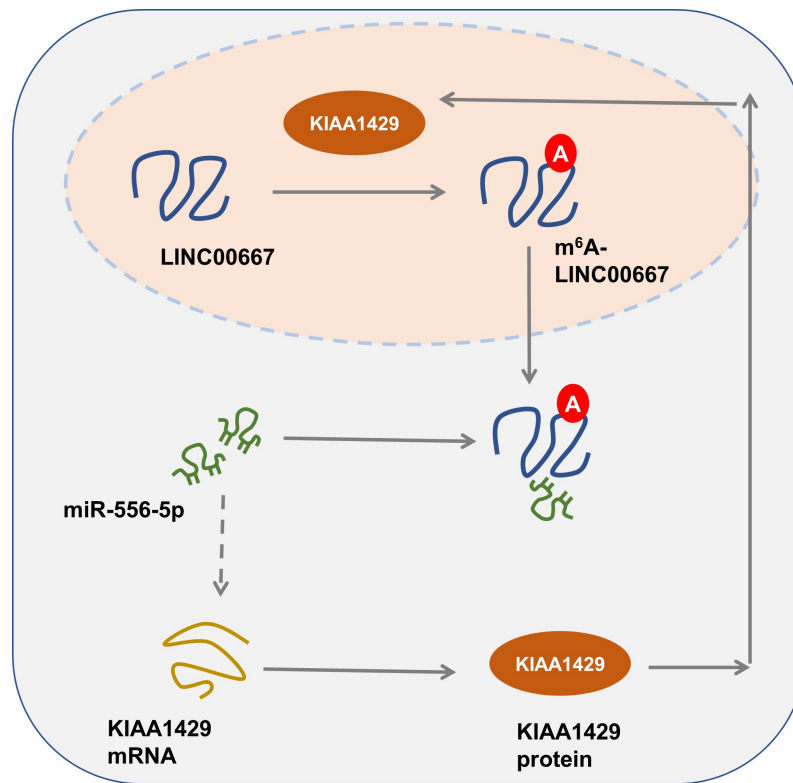


Figure 6. KIAA1429/LINC00667/miR-556-5p feedback loop promotes BC progression.

Tumorigenesis is a complicated multistep process involving cooperative activities of numerous genes, especially the activation of oncogenes and the inhibition of anti-tumor genes. In line with this notion, we found that LINC00667 exerted its oncogenic roles through positively regulating KIAA1429 via sponging miR-556-5p. Moreover, KIAA1429 could activate the stability of LINC00667 via m⁶A-dependent manner. In the vast majority of studies, lncRNAs directly or indirectly regulate their downstream target proteins through interacting with molecules, such as miRNAs or RNA binding proteins. For example, lncRNA HOTAIR is upregulated in invasive ductal carcinoma of breast cancer tissue, which promotes cell proliferation by regulating enhancer of zeste homolog 2 (EZH2) to Avian Myelocytomatosis Viral Oncogene Homolog (MYC) [20]. Therefore, the KIAA1429/LINC00667 acted a vital oncogenic element in m⁶A-dependent manner.

LINC00667 has been identified as an oncogene in other human cancers. For instance, in esophageal cancer, LINC00667 expression is up-regulated and LINC00667 knockdown represses the cell proliferation, migration, and invasion via miR-200b-3p/

SLC2A3 [21]. In cholangiocarcinoma, LINC00667 is highly expressed in tissues and cells, and the up-regulated LINC00667 is significantly associated with proliferation, migration, invasion, and epithelial-mesenchymal transition [22]. In Wilms' tumor, LINC00667 regulates cell viability and sphere formation ability, and competitively binds with miR-200b/c/429 to regulate IKK- β and then activates NF- κ B pathway [23]. Taken together, LINC00667 acted as an oncogene in human cancers, which was in accordance with existing evidence.

Due to the limitations of this research, we noticed that the rigorous relationship within KIAA1429 and LINC00667 needed further verification. Besides, the m⁶A modification on LINC00667 could inspire bigger opportunities in the future.

5. Conclusion

In conclusion, we found that m⁶A-modified LINC00667 was up-regulated in the BC tissue and cells. LINC00667 was positively activated by m⁶A methyltransferase KIAA1429 and synergistically regulated the BC cells' proliferation and

migration. LINC00667 positively regulated the KIAA1429 via sponging miR-556-5p, forming a KIAA1429/mA/LINC00667/miR-556-5p feedback loop. Collectively, the central findings of our study suggest that KIAA1429-induced LINC00667 exerted its functions as an oncogene in BC progression through m⁶A-dependent feedback loop.

Disclosure statement

No potential conflict of interest was reported by the author(s).

Funding

The author(s) reported that there is no funding associated with the work featured in this article.

ORCID

Xiliang Zhang  <http://orcid.org/0000-0002-1477-5945>

References

- [1] Co M, Liu T, Leung J, et al. Breast conserving surgery for BRCA mutation carriers—a systematic review. *Clin Breast Cancer*. 2020;20(3):e244–e50.
- [2] Dediu M, Zielinski C. A proposal to redefine pathologic complete remission as endpoint following neoadjuvant chemotherapy in early breast cancer. *Breast care*. 2020;15:67–71.
- [3] Marino MA, Avendano D, Zapata P, et al. Lymph node imaging in patients with primary breast cancer: concurrent diagnostic tools. *Oncologist*. 2020;25(2):e231–e42.
- [4] Mollon LE, Anderson EJ, Dean JL, et al. A systematic literature review of the prognostic and predictive value of PIK3CA mutations in HR(+)/HER2(-) metastatic breast cancer. *Clin Breast Cancer*. 2020;20(3):e232–e43.
- [5] Sauder CAM, Bateni SB, Davidson AJ, et al. Breast conserving surgery compared with mastectomy in male breast cancer: a brief systematic review. *Clin Breast Cancer*. 2020;20(3):e309–e14.
- [6] Guo L, Yang H, Zhou C, et al. N⁶-methyladenosine RNA modification in the tumor immune microenvironment: novel implications for immunotherapy. *Front Immunol*. 2021;12:773570.
- [7] Lu S, Ding X, Wang Y, et al. The relationship between the network of non-coding RNAs-molecular targets and N⁶-methyladenosine modification in colorectal cancer. *Front Cell Dev Biol*. 2021;9:772542.
- [8] Wang N, Yao F, Liu D, et al. RNA N⁶-methyladenosine in nonocular and ocular disease. *J Cell Physiol*. 2021;237(3): 1686–1710.
- [9] Wang Y, Li L, Li J, et al. The emerging role of m⁶A modification in regulating the immune system and auto-immune diseases. *Front Cell Dev Biol*. 2021;9:755691.
- [10] Chang G, Shi L, Ye Y, et al. YTHDF3 induces the translation of m(6)A-enriched gene transcripts to promote breast cancer brain metastasis. *Cancer Cell*. 2020;38(6):857–71.e7.
- [11] Ghafouri-Fard S, Hussien BM, Jamal HH, et al. The emerging role of non-coding RNAs in the regulation of virus replication and resultant cellular pathologies. *Int J Mol Sci*. 2022;23(2):815.
- [12] Mabeta P, Hull R, Dlamini Z. LncRNAs and the angiogenic switch in cancer: clinical significance and therapeutic opportunities. *Genes (Basel)*. 2022;13(1):152.
- [13] Zhao W, Geng D, Li S, et al. LncRNA HOTAIR influences cell growth, migration, invasion, and apoptosis via the miR-20a-5p/HMGA2 axis in breast cancer. *Cancer Med*. 2018;7(3):842–855.
- [14] Liang Y, Song X, Li Y, et al. LncRNA BCRT1 promotes breast cancer progression by targeting miR-1303/PTBP3 axis. *Mol Cancer*. 2020;19(1):85.
- [15] Chen DH, Zhang JG, Wu CX, et al. Non-coding RNA m⁶A modification in cancer: mechanisms and therapeutic targets. *Front Cell Dev Biol*. 2021;9:778582.
- [16] Yao ZT, Yang YM, Sun MM, et al. . In: *Cancer communications*. 2022;42(2): 117–140.
- [17] Zhao J, Lin X, Zhuang J, et al. Relationships of N⁶-methyladenosine-related long non-coding RNAs with tumor immune microenvironment and clinical prognosis in lung adenocarcinoma. *Front Genet*. 2021;12:714697.
- [18] Zhao C, Ling X, Xia Y, et al. The m⁶A methyltransferase METTL3 controls epithelial-mesenchymal transition, migration and invasion of breast cancer through the MALAT1/miR-26b/HMGA2 axis. *Cancer Cell Int*. 2021;21(1):441.
- [19] Huang T, Cao L, Feng N, et al. N⁶-methyladenosine (m⁶A)-mediated lncRNA DLGAP1-AS1 enhances breast cancer adriamycin resistance through miR-299-3p/WTAP feedback loop. *Bioengineered*. 2021;12(2):10935–10944.
- [20] Qian L, Fei Q, Zhang H, et al. LncRNA HOTAIR promotes DNA repair and radioresistance of breast cancer via EZH2. *DNA Cell Biol*. 2020;39(12):2166–2173.
- [21] Pan J, Zang Y. LINC00667 promotes progression of esophageal cancer cells by regulating miR-200b-3p/SLC2A3 axis. *Dig Dis Sci*. 2021. DOI:10.1007/s10620-021-07145-5
- [22] Li J, Guan C, Hu Z, et al. Yin yang 1-induced LINC00667 up-regulates pyruvate dehydrogenase kinase 1 to promote proliferation, migration and invasion of cholangiocarcinoma cells by sponging miR-200c-3p. *Hum Cell*. 2021;34(1):187–200.
- [23] Liu P, Chen S, Huang Y, et al. LINC00667 promotes Wilms' tumor metastasis and stemness by sponging miR-200b/c/429 family to regulate IKK-β. *Cell Biol Int*. 2020;44:1382–1393.